

Four-wave mixing in slow light photonic crystal waveguides with very high group index

Juntao Li,^{1,2} Liam O'Faolain,² and Thomas F. Krauss^{2,*}

¹State Key Laboratory of Optoelectronic Materials and Technologies, Sun Yat-sen University, Guangzhou, 510275, China

²SUPA, School of Physics and Astronomy, University of St Andrews, St Andrews KY16 9SS, UK
*tfk@st-andrews.ac.uk

Abstract: We report efficient four-wave mixing in dispersion engineered slow light silicon photonic crystal waveguides with a flat band group index of $n_g = 60$. Using only 15 mW continuous wave coupled input power, we observe a conversion efficiency of -28 dB. This efficiency represents a 30 dB enhancement compared to a silicon nanowire of the same length. At higher powers, thermal redshifting due to linear absorption was found to detune the slow light regime preventing the expected improvement in efficiency. We then overcome this thermal limitation by using oxide-clad waveguides, which we demonstrate for group indices of $n_g = 30$. Higher group indices may be achieved with oxide clad-waveguides, and we predict conversion efficiencies approaching -10 dB, which is equivalent to that already achieved in silicon nanowires but for a 50x shorter length.

©2012 Optical Society of America

OCIS codes: (190.4380) Nonlinear optics, four-wave mixing; (130.5296) Photonic crystal waveguides; (260.2030) Dispersion.

References and links

1. T. F. Krauss, "Slow light in photonic crystal waveguides," *J. Phys. D Appl. Phys.* **40**(9), 2666–2670 (2007).
2. T. F. Krauss, "Why do we need slow light?" *Nat. Photonics* **2**(8), 448–450 (2008).
3. T. Baba, "Slow light in photonic crystals," *Nat. Photonics* **2**(8), 465–473 (2008).
4. A. Yu. Petrov and M. Eich, "Zero dispersion at small group velocities in photonic crystal waveguides," *Appl. Phys. Lett.* **85**(21), 4866–4868 (2004).
5. L. H. Frandsen, A. V. Lavrinenko, J. Fage-Pedersen, and P. I. Borel, "Photonic crystal waveguides with semi-slow light and tailored dispersion properties," *Opt. Express* **14**(20), 9444–9450 (2006).
6. J. Li, T. P. White, L. O'Faolain, A. Gomez-Iglesias, and T. F. Krauss, "Systematic design of flat band slow light in photonic crystal waveguides," *Opt. Express* **16**(9), 6227–6232 (2008).
7. S. A. Schulz, L. O'Faolain, D. M. Beggs, T. P. White, A. Melloni, and T. F. Krauss, "Dispersion engineered slow light in photonic crystals: a comparison," *J. Opt.* **12**(10), 104004 (2010).
8. L. O'Faolain, S. A. Schulz, D. M. Beggs, T. P. White, M. Spasenović, L. Kuipers, F. Morichetti, A. Melloni, S. Mazoyer, J. P. Hugonin, P. Lalanne, and T. F. Krauss, "Loss engineered slow light waveguides," *Opt. Express* **18**(26), 27627–27638 (2010).
9. C. Monat, B. Corcoran, M. Ebnali-Heidari, C. Grillet, B. J. Eggleton, T. P. White, L. O'Faolain, and T. F. Krauss, "Slow light enhancement of nonlinear effects in silicon engineered photonic crystal waveguides," *Opt. Express* **17**(4), 2944–2953 (2009).
10. Y. Hamachi, S. Kubo, and T. Baba, "Slow light with low dispersion and nonlinear enhancement in a lattice-shifted photonic crystal waveguide," *Opt. Lett.* **34**(7), 1072–1074 (2009).
11. K. Inoue, H. Oda, N. Ikeda, and K. Asakawa, "Enhanced third-order nonlinear effects in slow-light photonic-crystal slab waveguides of line-defect," *Opt. Express* **17**(9), 7206–7216 (2009).
12. K. Suzuki and T. Baba, "Nonlinear light propagation in chalcogenide photonic crystal slow light waveguides," *Opt. Express* **18**(25), 26675–26685 (2010).
13. C. Monat, B. Corcoran, D. Pudo, M. Ebnali-Heidari, C. Grillet, M. D. Pelusi, D. J. Moss, B. J. Eggleton, T. P. White, L. O'Faolain, and T. F. Krauss, "Slow light enhanced nonlinear optics in silicon photonic crystal waveguides," *IEEE J. Sel. Top. Quantum Electron.* **16**(1), 344–356 (2010).
14. B. Corcoran, C. Monat, C. Grillet, D. J. Moss, B. J. Eggleton, T. P. White, L. O'Faolain, and T. F. Krauss, "Green light emission in silicon through slow-light enhanced third-harmonic generation in photonic crystal waveguides," *Nat. Photonics* **3**(4), 206–210 (2009).

15. V. Eckhouse, I. Cestier, G. Eisenstein, S. Combrié, P. Colman, A. De Rossi, M. Santagiustina, C. G. Smeda, and G. Vadalà, "Highly efficient four wave mixing in GaInP photonic crystal waveguides," *Opt. Lett.* **35**(9), 1440–1442 (2010).
16. J. F. McMillan, M. Yu, D. L. Kwong, and C. W. Wong, "Observation of four-wave mixing in slow-light silicon photonic crystal waveguides," *Opt. Express* **18**(15), 15484–15497 (2010).
17. C. Monat, M. Ebnali-Heidari, C. Grillet, B. Corcoran, B. J. Eggleton, T. P. White, L. O'Faolain, J. Li, and T. F. Krauss, "Four-wave mixing in slow light engineered silicon photonic crystal waveguides," *Opt. Express* **18**(22), 22915–22927 (2010).
18. J. Li, L. O'Faolain, I. H. Rey, and T. F. Krauss, "Four-wave mixing in photonic crystal waveguides: slow light enhancement and limitations," *Opt. Express* **19**(5), 4458–4463 (2011).
19. F. Morichetti, A. Canciamilla, C. Ferrari, A. Samarelli, M. Sorel, and A. Melloni, "Travelling-wave resonant four-wave mixing breaks the limits of cavity-enhanced all-optical wavelength conversion," *Nat Commun* **2**, 296 (2011).
20. B. Corcoran, M. D. Pelusi, C. Monat, J. Li, L. O'Faolain, T. F. Krauss, and B. J. Eggleton, "Ultracompact 160 Gbaud all-optical demultiplexing exploiting slow light in an engineered silicon photonic crystal waveguide," *Opt. Lett.* **36**(9), 1728–1730 (2011).
21. C. Xiong, C. Monat, A. S. Clark, C. Grillet, G. D. Marshall, M. J. Steel, J. Li, L. O'Faolain, T. F. Krauss, J. G. Rarity, and B. J. Eggleton, "Slow-light enhanced correlated photon pair generation in a silicon photonic crystal waveguide," *Opt. Lett.* **36**(17), 3413–3415 (2011).
22. C. Husko, T. D. Vo, B. Corcoran, J. Li, T. F. Krauss, and B. J. Eggleton, "Ultracompact all-optical XOR logic gate in a slow-light silicon photonic crystal waveguide," *Opt. Express* **19**(21), 20681–20690 (2011).
23. R. Salem, M. A. Foster, A. C. Turner, D. F. Geraghty, M. Lipson, and A. L. Gaeta, "Signal regeneration using low-power four-wave mixing on silicon chip," *Nat. Photonics* **2**(1), 35–38 (2008).
24. J. Li, L. O'Faolain, S. A. Schulz, and T. F. Krauss, "Low loss propagation in slow light photonic crystal waveguides at group indices up to 60," *Photon. Nanostruct.: Fundam. Appl.* in press., doi:10.1016/j.photonics.2012.05.006.
25. A. Gomez-Iglesias, D. O'Brien, L. O'Faolain, A. Miller, and T. F. Krauss, "Direct measurement of the group index of photonic crystal waveguides via Fourier transform spectral interferometry," *Appl. Phys. Lett.* **90**(26), 261107 (2007).
26. R. Lo Savio, S. L. Portalupi, D. Gerace, A. Shakoor, T. F. Krauss, L. O'Faolain, L. C. Andreani, and M. Galli, "Room-temperature emission at telecom wavelengths from silicon photonic crystal nanocavities," *Appl. Phys. Lett.* **98**(20), 201106 (2011).
27. T. Tanabe, H. Sumikura, H. Taniyama, A. Shinya, and M. Notomi, "All-silicon sub-Gb/s telecom detector with low dark current and high quantum efficiency on chip," *Appl. Phys. Lett.* **96**(10), 101103 (2010).
28. T. P. White, L. O'Faolain, J. Li, L. C. Andreani, and T. F. Krauss, "Silica-embedded silicon photonic crystal waveguides," *Opt. Express* **16**(21), 17076–17081 (2008).
29. L. O'Faolain, D. M. Beggs, T. P. White, T. Kampfrath, K. Kuipers, and T. F. Krauss, "Compact optical switches and modulators based on dispersion engineered photonic crystals," *IEEE Photonics J.* **2**(3), 404–414 (2010).

1. Introduction

The enhancement of nonlinear effects in slow light photonic crystal (PhC) waveguides is a topic of considerable current interest. Since the slow light effect increases the energy density in the waveguide, the light-matter interaction is enhanced considerably [1–3]. Using the additional tool of dispersion engineering, it is possible to control the group index, the dispersion and, to some extent, the loss [4–8]. A number of third-order susceptibility ($\chi^{(3)}$) effects have already been shown to benefit from slow light enhancement, such as self-phase modulation [9–13], which scales as S^2 , third-harmonic generation, which scales as S^3 [14], and four-wave mixing (FWM), which scales as S^4 [12,15–19] where S is the slowdown factor defined as the ratio between the group index and the phase index. In [18], for example, a FWM conversion efficiency of -24 dB was achieved for 90 mW continuous wave (cw) coupled input power in an engineered slow light silicon PhC waveguide of 396 μm length with a flat band group index of $n_g = 30$. Based on this and other successful demonstrations, many applications and novel effects, such as all-optical demultiplexing [20], correlated photon-pair generation [21], and all-optical XOR logic gate operation [22] have now been demonstrated, all benefitting from low input power and short waveguide length.

The stated S^4 enhancement, while applying in principle, is limited in practice by the effects of propagation loss and mode shape variation. We have already shown that other possible limitations, such as dispersive effects and nonlinear losses, are not an issue in engineered slow light silicon PhC waveguides [18]. Hence, the key strategy to achieving

higher conversion efficiencies, ideally approaching the value of ~ -10 dB for ~ 100 mW input pump power that has been reached by silicon nanowires [23], but now for much shorter (~ 2 orders of magnitude) length, is to increase the group index and to reduce the loss [18].

We now demonstrate FWM in a dispersion engineered slow light silicon PhC waveguide of $296 \mu\text{m}$ length with a flat band group index of $n_g = 60$. The waveguide is realized in an airbridge geometry in order to maximize the confinement and the operating window for dispersion engineering.

2. Fabrication and measurement

Waveguides of $296 \mu\text{m}$ length were fabricated on a SOITEC Silicon on Insulator (SOI) wafer, which comprised a nominally 220 nm thick Silicon layer on $2 \mu\text{m}$ of silica. In order to implement the dispersion and loss engineering techniques for 1550 nm operation, we used a lattice period of $a = 412$ nm, a hole radius of $r = 120$ nm, and shifted the first and second hole along the waveguide by $s_1 = -42$ nm and $s_2 = 20$ nm, respectively (positive values indicate a shift away from the waveguide) [6, 8, 24]. On-chip inverse taper mode converters with SU8 polymer waveguides were added to achieve a 40% injection efficiency from free space to the PhC waveguide [18].

The experimental setup of the dispersion and FWM measurement is shown in Fig. 1. The setup combines an interferometric slow light setup [25] with an FWM measurement [18]. We use an amplified spontaneous emission (ASE) broadband source and a Mach-Zehnder interferometer (MZI) that consists of two 50:50 fiber couplers in order to measure the transmission and dispersion of the waveguide [25]. In the blue portion of Fig. 1, a tunable cw laser is amplified by an EDFA ($P_{\text{max}} = 600$ mW) and acts as the pump for the FWM measurement, while a fixed wavelength cw polarization maintaining DFB laser diode acts as the probe signal. The maximum coupled pump power inside the PhC waveguide is estimated to be 90 mW [18].

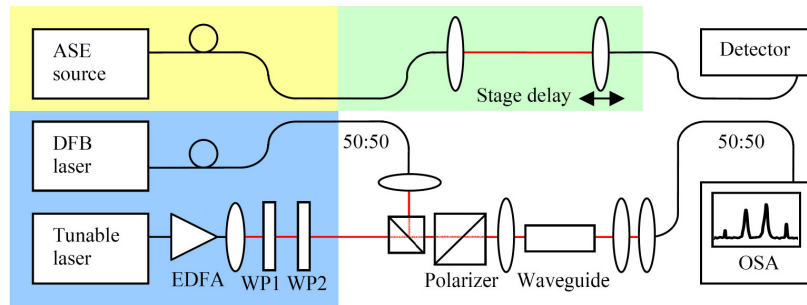


Fig. 1. Schematic setup of the dispersion and FWM experiment. The yellow part is the ASE source which is used for the transmission and slow light measurement of the waveguide. The green part is the reference arm of the slow light measurement MZI. The blue part is the pump (tunable laser and EDFA) and probe (DFB laser diode) source of the FWM measurement. WP1 and WP2 are quarter- and half-wave plates, respectively, that are used to control the polarization of the cw pump laser.

The measured group index n_g and the transmission of the waveguide are shown in Fig. 2. For this measurement, the pump and probe sources for the FWM experiment (blue part of Fig. 1) was blocked. A constant group index of $n_g = 60$ was achieved with a 4 nm low loss bandwidth around 1550 nm. The propagation loss in the slow light region was measured to be 130 dB/cm via the cutback method [24].

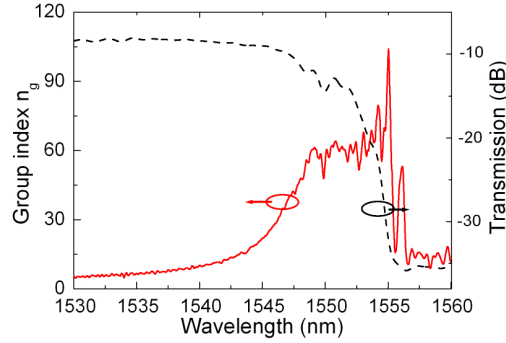


Fig. 2. Measured transmission spectrum (black dashed line) and group index (red solid line) of the engineered slow light PhC waveguide with spot size mode converter.

The FWM efficiency was measured by adding the pump and probe power (blue portion of Fig. 1) and blocking the reference arm of the slow light measurement MZI (green part of Fig. 1). The influence of the ASE source on the FWM measurement can be ignored because the spectral power density of the ASE source is much lower than that of the pump and probe. Figure 3(a) shows the experimentally measured FWM conversion efficiency as a function of the coupled input pump power and compares it to simulations. The results for the engineered slow light waveguide of 296 μm length and $n_g = 60$ were compared to those of a silicon nanowire of the same length and $n_g = 4$. All three wavelengths, i.e. pump (1550.4 nm), probe (1550.1 nm) and idler (1550.7 nm) were positioned in the flat band slow light region to ensure uniform enhancement. The simulation results were based on the analysis and parameters in [18].

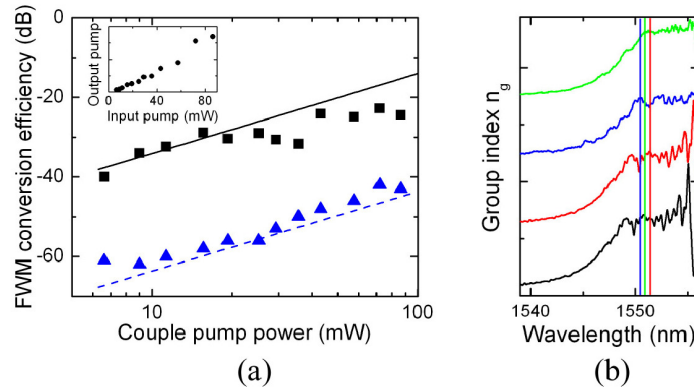


Fig. 3. (a) Experimental (Dots) and calculated (lines) results of the FWM conversion efficiency vs. the coupled input pump power in an airbridge engineered slow light PhC waveguide ($n_g = 60$, black) and a nanowire ($n_g = 4$, blue) of same length (296 μm). Inset: Output pump power as a function of the input pump power up to 90 mW, highlighting the absence of nonlinear absorption (b) Dispersion curve of the engineered slow light PhC waveguide for different coupled pump powers of 0 mW (black), 15 mW (red), 35 mW (blue) and 90 mW (green). The color lines represent the positions of the three wavelengths involved in the FWM process.

For completeness, we define the FWM conversion efficiency as the ratio between the idler power on the output side and the probe power on the input side of the structure [18], which is the definition used by most groups working in the field:

$$\eta = \frac{P_{\text{idler}}(L)}{P_{\text{probe}}(0)} = S^4 \gamma^2 \bar{P}_{\text{pump}}^2 L^2 e^{-\alpha L} \varphi, \quad (1)$$

where S is the slowdown factor, $\gamma = 2\pi n_{2\text{eff}} / (\lambda \cdot A_{\text{eff}})$ is the material nonlinear parameter, $n_{2\text{eff}}$ is the effective nonlinear index of silicon, A_{eff} is the effective cross-section mode area, $\bar{P}_{\text{pump}} = P_{\text{pump}}(0) \times (1 - \exp(-\alpha L)) / \alpha L$ is the path average pump power, α and L are the loss and physical length of the structure, and ϕ is the phase factor. At low power, we note a close agreement between theory and experiment and observe a difference of 30 dB between the PhC waveguide and the nanowire. This is expected from the difference in group index and effective mode area according to Eq. (1): the group index of the slow light waveguide is 15 times higher, while the mode area is 5 times lower, resulting in a ratio of $15^4/5^2 = 33$ dB, with the 3 dB difference arising from propagation losses.

The FWM conversion efficiency for 15 mW coupled pump power is -28 dB, which is quite a remarkable value for such a low pump power. Increasing the power does not result in much further improvement, however, and we note that the efficiency curve saturates with a maximum value of -22 dB observed for 75 mW coupled pump power. This saturation is in contrast to the expected value of -14 dB predicted for 100 mW coupled pump power, which would be an outstanding result, especially for this waveguide length and pump power. The immediate concern is that the power is limited by nonlinear effects such as two photon absorption, but as shown in the inset of Fig. 3(a), the relationship between input and output power remains linear throughout the entire power range investigated here, highlighting that the observed saturation is not caused by nonlinear losses.

Instead, we believe that thermal effects are responsible for the observed saturation. Defect luminescence has been observed from this material [26] implying that the absorption does occur in silicon PhCs. This was also observed in [27]. Given the high energy density in the waveguide at maximum group index and the fact that we use an airbridge geometry, which is thermally isolated, even this very weak absorption is sufficient to lead to significant heating, detuning the waveguide. As shown in Fig. 3(b), we observe a maximum shift of 2.5 nm for 90 mW coupled input power, which corresponds to $\Delta T \approx 25^\circ$ C. Correspondingly, the pump, probe and idler waves are no longer all positioned in the flat band slow light region and the FWM conversion efficiency is reduced. This interpretation is confirmed by the fact that previous work on similar waveguides, but with much higher peak power (≈ 10 W) and conducted in the pulsed regime [17] did not show any evidence for such a shift.

3. Discussion and improvement

An obvious solution to the thermal problem is to embed the waveguide in a material with higher thermal conductivity, such as silica. Since the thermal conductivity of silica is 50 times larger than that of air, oxide-clad PhC waveguides [28] can overcome the thermal limitation. Additionally, oxide-cladding has the advantage of passivating the sidewalls to some extent, thus reducing the very origin of the linear losses, namely surface defects.

In order to demonstrate this solution, we designed and fabricated an oxide-clad dispersion engineered slow light silicon PhC waveguide with a group index of $n_g = 30$ and 12 nm bandwidth [29] by spinning flowable oxide (FOX-14 from Dow Corning) onto the PhC waveguide structure after the silicon etch. The device was not membraned, i.e. the original buried oxide layer was still in place. This leads to a very small index asymmetry (buried oxide has a slightly higher index than the spin-on glass), but previous investigations [28, 29] have shown that this has no apparent impact. We have also demonstrated that the loss of buried oxide waveguides in the slow light regime is comparable to that of airbridges. The only disadvantage is the reduced parameter space for dispersion engineering, due to the lower refractive index contrast; hence it is more difficult to achieve the high group index of $n_g = 60$ demonstrated above. As a result, we performed the experiment on $n_g = 30$ waveguides.

The FWM results obtained with these oxide clad waveguides are shown in Fig. 4, and are compared to airbridge engineered slow light waveguides of the same length ($L = 396 \mu\text{m}$),

operating at the same group index ($n_g = 30$) [18]. The similarity is underlined by the -24 dB conversion efficiency for 90 mW coupled input pump power. The dispersion curves and the cutoffs in transmission of these two waveguides are also shown in Fig. 4 to compare the red shifts in the slow light region. For the airbridge waveguide, the red shift in the slow light region was smaller for $n_g = 30$ than $n_g = 60$, as expected, while the red shift is almost non-existent for the oxide-clad waveguide. Because of the wide bandwidth (13 nm) of the slow light region with the lower group index of 30, this red shift did not influence the linear relationship between the FWM conversion efficiency and the pump power and the conversion efficiency is maintained. Figure 4 confirms the possibility of using oxide-cladding to overcome the thermal detuning observed in airbridge waveguides at high cw input powers.

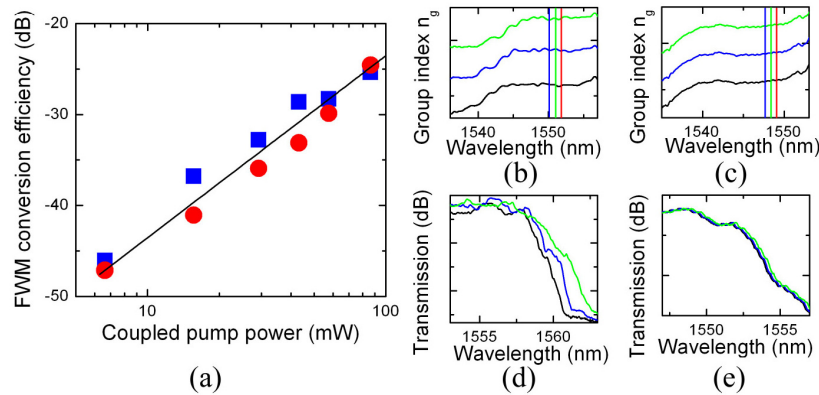


Fig. 4. (a) Experimental (dots) and calculated (lines) values of the FWM conversion efficiency as a function of coupled input pump power in airbridge (blue square dots) [18] and oxide-clad (red circle dots) engineered slow light PhC waveguides of $396 \mu\text{m}$ lengths with a group index of $n_g = 30$. (b)(c) Group index curves and (d)(e) transmissions for (b)(d) airbridge and (c)(e) oxide-clad waveguides for coupled pump powers of 0 mW (black), 35 mW (blue) and 90 mW (green). The color lines in (b)(c) represent the position of the pump, probe and idler of the FWM process.

4. Conclusion

We have shown that a relatively high FWM conversion efficiency of -28 dB is possible in a slow light PhC waveguide, using a coupled cw input power of only 15 mW. The waveguide is $296 \mu\text{m}$ long and exhibits a constant group index of $n_g = 60$ over a useful bandwidth of $\Delta\lambda = 4$ nm. Somewhat surprisingly, we also observe a thermal detuning of the waveguide for higher input power, which we associate with heating due to linear losses at surface defects and the high energy density in the slow light regime. By embedding the waveguide in silica, we show that this issue can be addressed based on the passivation and the much better thermal conductivity provided by the silica overlayer. Since embedding the PhC in silica reduces the refractive index contrast, it is more difficult to achieve high group index operation ($n_g > 50$), but once such designs are available, we are confident that conversion efficiencies approaching -10 dB can be achieved with waveguides of only a few $100 \mu\text{m}$ in length. The compact geometry of slow light PhC waveguides and the mechanical stability provided by the oxide cladding allows much tighter integration and improves the CMOS compatibility of PhC devices for optical signal processing.

Acknowledgment

This work was supported by the EPSRC - UK Silicon Photonics consortium. Dr. J. Li was supported by EU-FP7 Marie Curie Fellowship project "OSIRIS" and "985 project" of Sun Yat-sen University. The fabrication was carried out in the framework of the NanoPix platform (www.nanophotonics.eu).